Chapter 6

Photonic Sensors Based on Flexible Materials with FBGs for Use on Biomedical Applications

Alexandre Ferreira da Silva, Rui Pedro Rocha, João Paulo Carmo and José Higino Correia

Additional information is available at the end of the chapter

http://dx.doi.org/10.5772/52974

1. Introduction

A wide variety of optical fiber sensors are available and can be divided into three categories: the external or extrinsic ones (Beard P. C. et al., 1996) where the fiber is only used to drive the measured information to and from the transducer at a distant location, the intrinsic category (Boerkamp M. et al., 2007) where the optical properties are sensitive to an external stimulus (Grattan S. K. T. et al., 2009; Gu X. et al., 2006), and the hybrid category where the light is transferred over the optical fiber for conversion into electricity on a distant optical receiver (Yao S.-K. et al., 2003).

From the previously mentioned categories, the intrinsic sensors, where FBGs are included, have been studied and applied intensively during the past 20 years (Lee B., 2003). The Bragg grating structure is the intrinsic element to the fiber responsible for the sensor behavior. The gratings can be inscribed by ultraviolet (UV) light beams, taking advantage of the optical fiber photosensitivity (doped with germanium) to this radiation. In addition to the standard advantages attributed to the optical fiber sensors, FBGs have an inherent self-referencing and multiplexing capability. Essentially, the FBG is a periodic variation of the refraction index along the fiber axis. As illustrated in the Figure 1, this structure works as a reject-band filter, reflecting back the spectral component, λ_B [nm], which satisfies the Bragg condition (given by equation (1)) and transmitting the remaining components. The Bragg wavelength is given by (Hill K. O. et al., 1997):

$$\lambda_B = 2n_{eff}\Lambda \tag{1}$$

where Λ [nm] is the grating pitch and n_{eff} is the effective refraction index of the fiber core. The wavelength shift, $\Delta\lambda_B$ [nm], of a FBG sensor subject to a physical disturbance is given by (Wei C.-L. et al., 2010):

$$\frac{\Delta\lambda_B}{\lambda_B} = (1-\rho_e)\Delta\varepsilon + (\alpha+\xi)\Delta T \tag{2}$$

where ρ_e, $\Delta\varepsilon$, α, ξ, and ΔT are the effective photoelastic constant, the axial strain, the thermal expansion, the thermal optic coefficient and the temperature shifts, respectively. The ratio in the first term of equation (2) expresses the strain effect on an optical fiber. It corresponds to a change in the grating spacing and the strain-optic induced change in the refractive index. The temperature sensing is mainly related with the second term of the expression. As the FBG is subjected to temperature variation, it dilates or contracts, modifying the grating pitch.

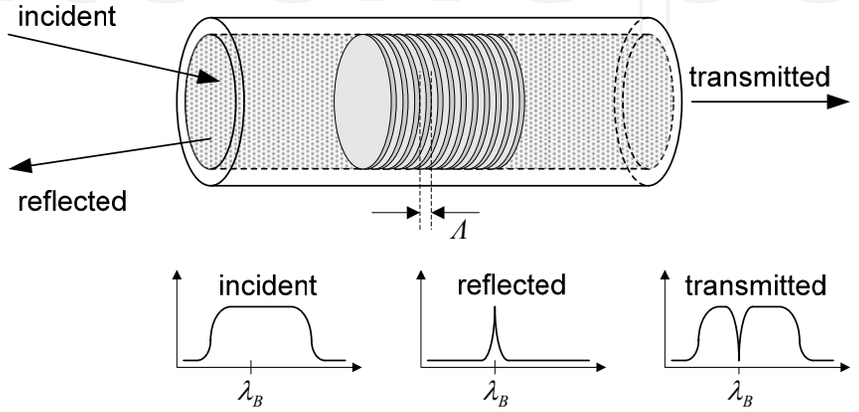

Figure 1. Illustration of working principle of FBGs.

One main advantage of this system is the measurements made on the wavelength instead of optical power. This enables a system that is not sensitive to external factors as fluctuations of the optical source. The stability is also extended to the bond between the polymer matrix and the optical fiber in which it is wrapped. Therefore, these features make the FBGs suitable sensing elements for doing physical measurements, where a kind of displacement is available. Examples of such applications found in the literature include the measurements of strain (Grattan S. K. T. *et al*., 2009; Ling H. Y. *et al*., 2006), pressure (Peng B. J. *et al*., 2005; Zhang W. et al., 2009), force (Rajan G. *et al*., 2010; Zhao Y. *et al*., 2005), tilt rotation by an angle (Peng B. J. *et al*., 2006; Xie F. *et al*., 2009), acceleration (Antunes P. *et al*., 2011; Fender A. *et al*., 2008), temperature (Bao H. *et al*., 2010; Gu X. *et al*., 2006), humidity (Arregui F. J. *et al*., 2002; Yeo T. L. *et al*., 2005), magnetic fields (Orr P. *et al*., 2010), cardiorespiratory function (Silva A. F. *et al*., 2011a), hand posture analysis (Silva A. F. *et al*., 2011b), gait function analysis (Rocha R. P. *et al*., 2011) and integration on wearable garments (Carmo J. P. *et al*., 2012).

This chapter focuses on biomedical applications of FBGs embedded into flexible carriers for enhancing the sensitivity and protection to the optical fiber, and to provide interference-free instrumentation. The same FBG system was used in all experiments presented in this chapter. In terms of construction, this FBG system is composed by a sensing and a monitoring module. Figure 2 shows photographs of the light source and the hardware used in the interrogation system for monitoring the received light which is then seen on a computer screen. The Fiber-Bragg Grating used in these experiments was produced by the FiberSensing company (FiberSensing, 2012). The grating is 8 mm long with a resonance

wavelength in the 1550 nm range, which corresponds to a refraction index modulation period of the core in the half-micrometer range. The interrogation monitor (I-MON 80D from Ibsen Photonics company (Ibsen, 2012) allows real-time spectrum monitoring of FBG sensors interrogation systems. Along with the interrogation monitor, software is supplied by the manufacturer that permits real-time visualization of the waveforms while the sensor is being actuated. This system has a resolution of 10 pm.

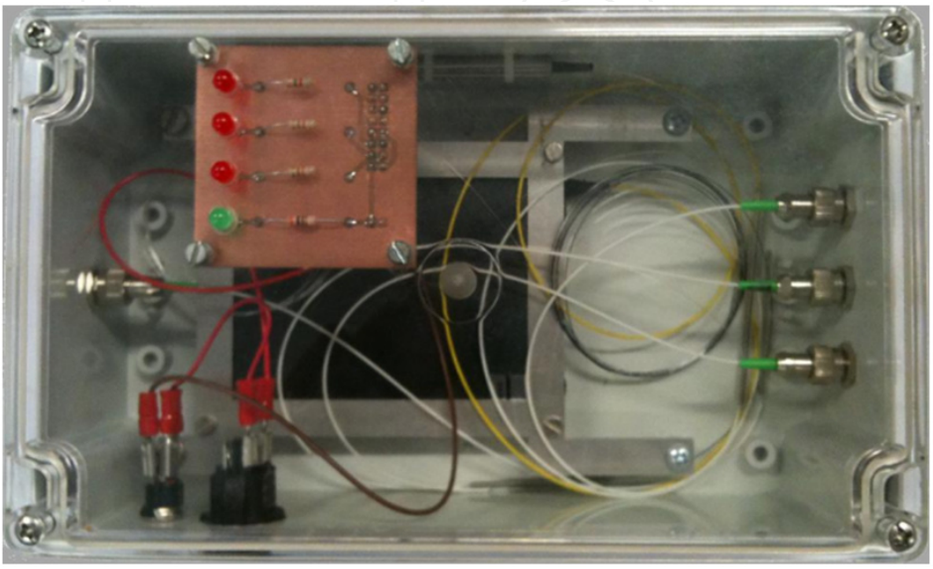

(a)

(b)

Figure 2. Proposed system's non-sensing parts composed by (a) broadband light source (Denselight, 2012) and in (b) the optical circulator (Oplink, 2012) and interrogation monitor hardware (Ibsen, 2012).

A carrier material made of polychloroethanediyl (polyvinyl chloride, or simply PVC) was used in the FBG embedment for increasing their sensitivity to strains and at the same time to improve the adhesion to the surface under measurement (Silva A. F. et al., 2012). The PVC

material was selected as FBG carrier due to its excellent performance/cost ratio and easy handling during the manufacturing process. Moreover, the PVC presents many other advantages when compared with its direct competitors (e.g., either the polyurethane or the polyolefin) such as low production cost, making this material highly competitive. On the practical side, it offers high resistance to aging, high versatility and simplicity of maintenance (Silva A. F. et al., 2012). The cross-sections of the Figure 3 show the configuration of the layers within the carrier (few photographs was taken under different directions and illuminations for better illustrating the FBGs and layers that constitute the carrier).

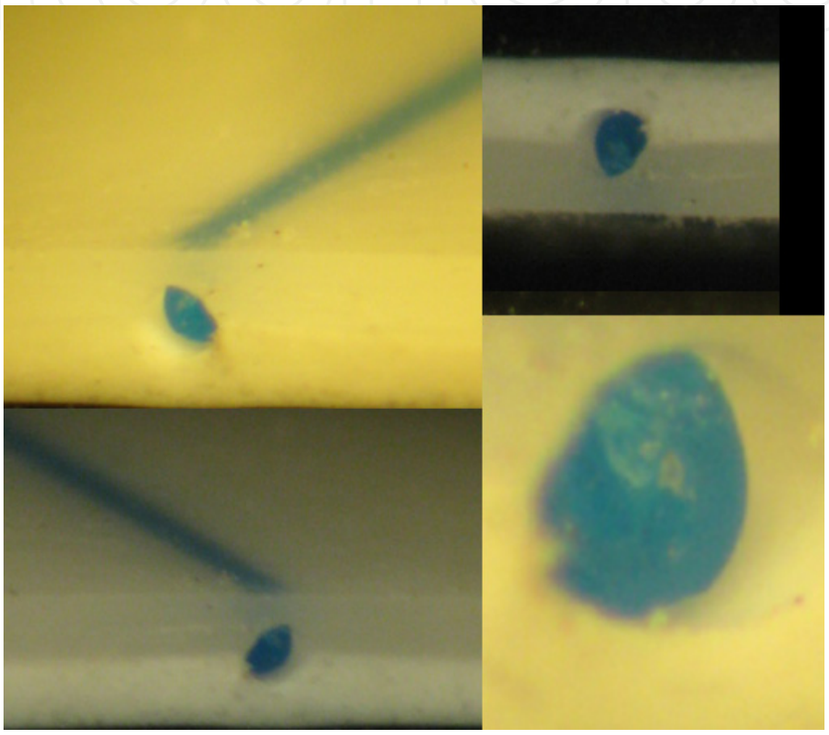

Figure 3. Few photographs showing views with the cross-section of the three layers that constitutes the carrier. The supported FBGs are also showed.

2. Knee's kinematic monitoring

2.1. Introduction

In this section of the chapter is presented a sensing electronic-free wearable solution for monitoring the knee-referenced gait process as a biomedical application example using Fiber Bragg Grating (FBGs) sensors. This sensing system is based on a single optical FBG, with a resonance wavelength of 1547.76 nm, which shifts to lower or higher wavelengths when subjected to strain variations, with a resolution of 10 pm. The measuring of the knee movements, flexion and extension with the corresponding joint acting as the rotation axis, is shown for a healthy individual. The optical fiber with the FBG is placed inside a polymeric foil (composed by three flexible layers), attached to an elastic knee band, which facilitates its placement in the knee (centered in the patella) while maintaining full sensing capabilities. Although the knee is used here as the example, the way the device is placed on the specific

body part to be measured enables the clear detection of the movements in respect to the corresponding joint. The proposed prototype was evaluated under different condition tests and also to assess its consistency and flexibility of use. The designed sensor demonstrates advantages in biomedical fields such as physical therapy and athletic assessment applications because of the system's resolution and easiness of applying it onto the body part under investigation. Another advantage is the possibility to measure, record and evaluate specific mechanical parameters of the limbs' motion. Patients with bone, muscular and joint related health conditions, as well as athletes, are within the most important end-user applications. Moreover, this system can be used simultaneously with, for example, inertial and magnetic sensors enabling the correlation between the measured wavelengths with angular degrees.

During the past years, body kinematics monitoring in human beings is a growing area within the field of engineering applied to medicine. Universities, high-performance sport centers and health-care institutions have been developing ways to accurately measure and evaluate the way the human body moves for endless purposes. The main objectives for such attention in measuring and evaluating the human body kinematics are improvements of athletic performance (Anderson D. et al., 1994; Yamamoto Y., 2004; von Porat A. et al., 2007) in competitions and historic evaluation studies of patients to determine if the prescribed therapy is being efficient and evaluating the rehabilitation of patients (Yang X. J. et al., 2012; Vancampfort D. Et al., 2012; Cup E. H. et al., 2007; Kun L. et al., 2011) based on the information provided by measuring the limbs' movements. Several systems for body kinematics monitoring have been realized using different approaches such as complex electronic systems including a 2.4 GHz radio-frequency (RF) transceiver (Afonso J. A. et al., 2010), motion capture techniques (Ren L. et al., 2008; Parker T. M. et al., 2008) and advanced software algorithms that demand profound specific know-how and are also very complex (Moustakidis S.P. et al., 2010; Wu Y. et al., 2011). Other applications for limb posture monitoring include the assessment of certain neurologic and orthopedic diseases (Yavuzer G. et al., 2008; Mavrogiorgoua P. et al., 2001; Turcot K. et al., 2008). A gait monitoring system based on optical fiber, complemented with a motion capture system, has already been proposed but, when compared to the solution presented in this paper, it shows several differences including: use of a plastic optical fiber (POF), calibration procedure required and measurement based on the transmitted optical power when the POF is bent (Bilro L. et al., 2011). Therefore, the importance of measuring (Godfrey A. et al., 2008) and characterizing the limbs' kinematics is quintessential in diagnosing physical and mental disorders, originated by trauma, stroke or disease, and determining the appropriate treatment and therapy. The data can be saved (using the setup showed in the Figure 2) for further analysis and study which enables comparisons between results to be made along the time. Moreover, the proposed system was designed to obtain maneuverability making it compatible with free range body kinematics movements.

2.2. Approach

The gait cycle can be defined as the sum of the two components that compose a full step, *e.g.* the stance and the swing phases. The stance and swings phases comprehend the periods when the foot is touching the ground and advancing in the air permitting the progression of

(a)

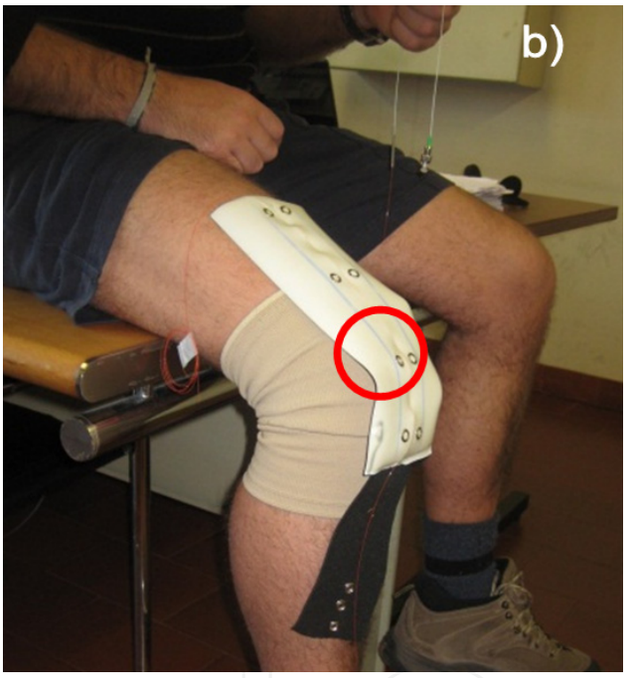

(b)

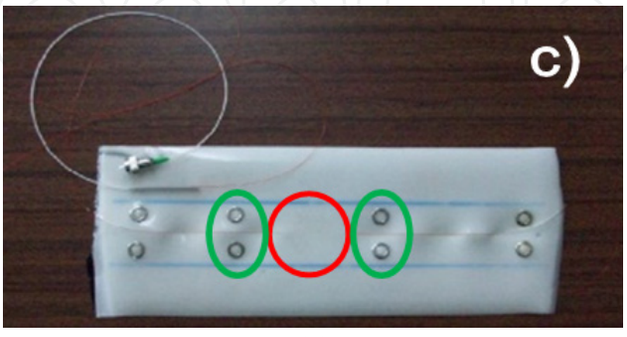

(c)

Figure 4. In (a), the elastic knee with the pressure buttons signaled with green ellipses. In (b), the sensing part attached to a standard elastic knee band and in (c), a close-up just of the PVC foil with the embedded FBG signaled with a red circle and the pressure buttons with green ellipses.

the body, respectively. The knee kinematics is represented by two stages: flexion and extension. The objective is to represent graphically, as a function of the measured wavelength, the full human gait period, centered on the knee joint using just one FBG and a single mode optical fiber. This section focus on the validation of the proposed concept by measuring the knee's kinematics, the single fiber and single FBG sensor, placed in the center of the knee (patella), are enough to measure and evaluate the subject's evolution. In order to make this possible, a high-sensitivity sensor is necessary to detect the full movement from one extreme (when the leg is completely straight) to the other (maximum knee deflection during gait) and all movements that happen in-between, *i.e.*, stance and swing phases. The sensing part is based on a flexible structure that can be placed/removed on/from the knee very easily. This is done by using small pressure buttons as attaching elements. The Figure 4 shows in more detail the small metallic pressure buttons that attach the different components of the sensing system, the elastic knee band already placed and the foil with the embedded FBG. This type of elastic knee band is regularly used in prevention/precaution situations in people with a temporary or permanent muscular injury enabling the use of the flexible structure by any person and in any junction in the body. The pressure buttons ensure that the sensing element is able to sense the flexion and extension of the knee as the subject moves around. Since optical fibers are immune to electromagnetic interference (EMI) and can be used safely in wet environments or even under water, the proposed solution increases the number of possible applications for this technology.

2.3. Flexible sensing structure

The accurate measurement of the knee joint movement is possible if the dynamic range of the sensor is increased. This can be accomplished by proper selection of the substrate material that can conform correctly to the actual movement. Therefore, a structure with enough area to cover the knee enables the transference of the movements to the embedded sensor. A wide rectangular configuration was chosen to cover both the flexion and the extension movements since it provides the required area of contact to be translated by the sensing area and allows the light to travel without any abrupt corners that would obstruct the communication with the monitoring stage. The main characteristics, and advantages, of this foil include flexibility, stretchability and the capability to sustain a good bonding between the optical fiber and the substrate. The host material is polyvinyl chloride (PVC) with custom formulation to assure the bonding and the stimulus transfer (Silva A. et al., 2012). Moreover its size and shape are completely customizable during fabrication.

2.4. Samples and experiments

As previously stated, the knee kinematics is characterized mainly by the flexion and extension dynamics. In order to monitor these movements, the flexible polymeric foil prototype, having the sensor embedded in it, was applied to an elastic knee band placing the FBG correctly on the patella using pressure buttons as bonding elements. The Figure 5 shows the raw data measured by the FBG with the volunteer walking and running on top of a commercially available treadmill validating the system's consistency and reliability.

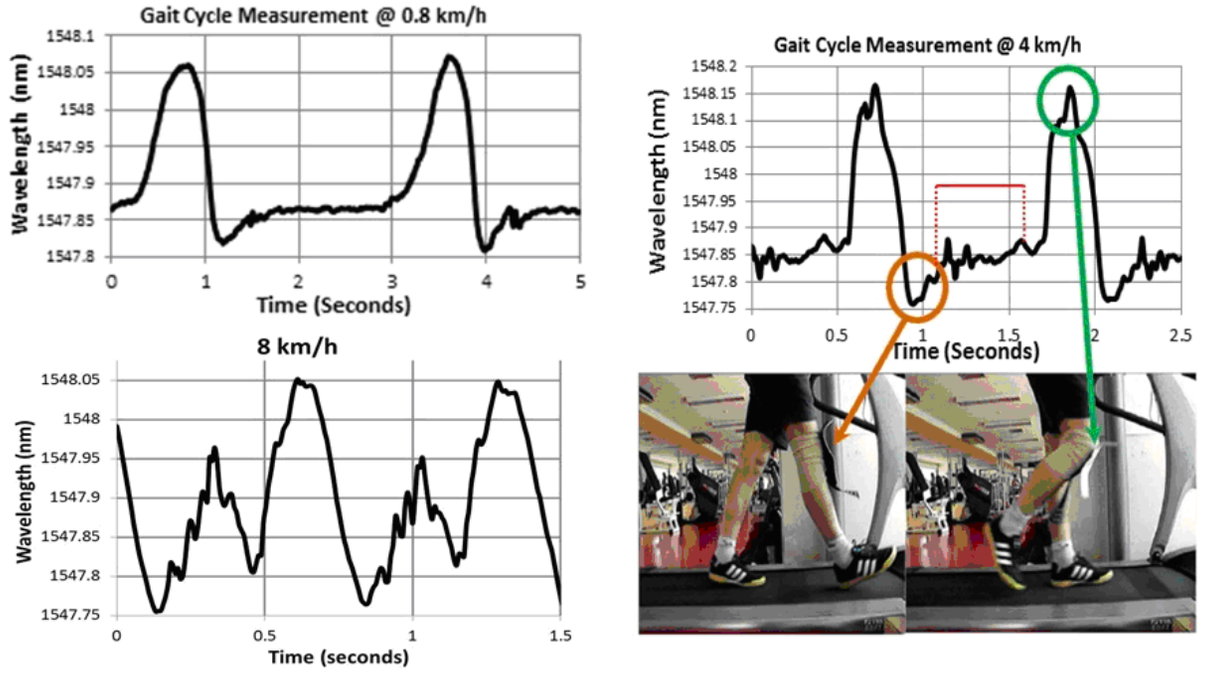

Figure 5. FBG's measured raw unfiltered two full gait cycles for three different speeds. Key points of the swing and stance phases are represented by the minimum and maximum deflections of the FBG, and the time in-between them, respectively.

The periodicity of the signals and the respective association with the gait cycle are easily recognized, *i.e.*, all the different movements associated with a full step are clearly identifiable in the measured waveforms. The tests were done during 10 seconds but only two full gait cycles are considered for clear visualization of the acquired raw unfiltered data. In the Figure 5 it is seen the FBG's raw data waveforms for three different walking speeds, as an example of the system's capability, at 0.8 km.h^{-1} (0.22 m.s^{-1}), 4 km.h^{-1} (1.11 m.s^{-1}) and 8 km.h^{-1} (2.22 m.s^{-1}). For the highest speed, the measured curve becomes sharper with few differences. The running movement is a quicker step which leads to the waveform sharpness and presents a slight different kinematics, mainly when the front foot reaches the ground and pulls the entire body forward. Nonetheless, the results enable the identification of the several events occurring during the walking and running movements. In order to compare the period of the measured data with the different stages of a full step, the Figure 5 shows the two extreme values obtained by the system during a complete step on a 2.5 seconds measurement at 4 km.h^{-1}. The stage where the flexion of the leg in the knee joint, hence on the FBG as well, is the minimum possible during a full step is visible corresponding to a value of 1547.76 nm (resonance wavelength). The maximum deflection obtained during a step corresponds to a value of 1548.16 nm. Between the two extremes of the movement, there is a stage with low amplitude variations that follows the knee movement while the leg is in contact with the floor. It should be noted that between the minimum and maximum values, the leg is always touching the floor (stance phase) and the FBG sensor is basically completely stretched with just minor variations related to the elastic knee band used. This relatively constant period is marked in red in the chart seen in the Figure 5. The right leg starts its movement backwards touching the floor first with the ankle,

proceeding with the base of the foot until it begins the movement forward with the tip of the toes (the maximum deflection represented in the figure represents around 80% of the gait period (Trew M. et al., 2005). The FBG based sensor enables identification of all the different movements associated with a full step allowing comparison between different results acquired in different situations. The presented solution for the knee can also be applied to any other joint in the human body.

2.5. Discussion

The measurements seen in Figure 3 show a smooth waveform at low speeds. For speeds above 4 km/h the elasticity factor of the knee band and the slip occurring during the movement change slightly the position of the attached FBG in the knee-band. It can be concluded that the elastic band matches perfectly the skin for slow movements (roughly≤4 $km.h^{-1}$) guaranteeing that the FBG is always on the correct place. Due to the FBG's high resolution, 10 pm, the slightest slip induces immediately a change in the output data. This means that a "calibration" procedure is needed to guarantee that the sensor is exactly on top of the patella. Also, the elastic band used is specified for a leg perimeter around the knee of 35-38 cm. For the subjects with a corresponding leg girth, it reproduces correctly the knee movement during the gait. For the remaining ones, a slight displacement of the FBG occurs due to the vibration induced in the leg while taking steps forward, and therefore explaining the wavelength variations observed in the measurements. Typically, the knee position tends to be steady at low speeds as seen in the test performed at 0.8 $km.h^{-1}$ in the Figure 5, but its variations become more significant as the speed increases. The stronger vibration caused by the running steps is the source for the somewhat abrupt peaks in the waveform at 8 $km.h^{-1}$. Different sizes of the elastic knee band and the way it is attached to the foil with the embedded sensor or even embed it in the textile (Grillet A. et al., 2008) of an elastic knee band can also reduce these fast oscillations. Regarding the sensing electronic modules, the fast changes observed can also be explained.

2.6. Conclusions

A structure made of polyvinyl chloride (PVC) material, carrying an embedded Fiber Bragg Grating (FBG) sensor with a 10 pm resolution, was attached to an elastic knee band. A clear characterization of the movement of the knee joint as a function of the wavelength variation and the associated angle measured between the tibia and femur were obtained. All the different movements associated with a full step, the stance and swing phases and their characteristic progression, are clearly identifiable in the obtained waveforms allowing comparison between different results acquired in different situations. The presented prototype is easy to connect and does not require technical personnel to give support and expertise making this approach very interesting as a functioning system for body kinematics monitoring. Moreover, since optical fiber is immune to electromagnetic interference and can support wet environments, including under water, the developed system opens new applications for body kinematics monitoring when a direct and easy relation between wavelength variation and angles is achieved. The FBG really demands a careful placement,

and for walking speeds above 4 $km.h^{-1}$, the knee band slips and does not reproduce as accurately the gait cycle. Another solution for this problem could be to embed the optical fiber with the sensor in the actual textile to be used on the knee. The integration of a single optical fiber in a polymeric foil made of PVC resulted in a structure with a very good sensitivity for transducing accurately the knee flexion and extension during the walking and running tests. It is easy to install, comfortable to wear and accurately measures the body kinematics. Since this approach uses a flexible structure it can be worn by any person and it can be applied to other articulations as the shoulder or the elbow.

3. Hand posture monitoring

Following the knee's kinematics monitoring example, the FBGs can be used in more tricky examples as the hand posture monitoring. In reality, the FBG is a powerful tool for monitoring the body articulations due to its sensitivity, response and inherently properties as multiplexing.

The hand is possibly on the most complex articulating system mainly due to the density of articulations per volume. Moreover, apart from the anatomic structure, the hand is a key element to perform the interface between the human and the world. One could imagine how difficult it would be to perform its daily duties without using any hand.

However, the hand impairment is more common that one could image, mainly driven by stroke. Just in 2010, 73.7 billion dollars (Lloyd-Jones D. et al., 2010) were mainly spent on rehabilitation programs required to minimize muscle spasticity or pain and to recover from impairment. It is on this very stage that FBGs can be a great tool not only to enhance the rehabilitation programs but also to minimize their costs.

3.1. Hands' kinematics

The hand movements can be simplified to flexion-extension (straightening of the fingers) and abduction-adduction (pulling fingers apart or towards each other).

In today's physical therapy sessions, the exercises focus mainly on finger passive range of motion, fist making, object pick-up, finger extension and grip strengthening. In reality, one is mainly performing flexion-extension movements, which is the most frequently performed movement on a daily basis. Furthermore, the abduction-adduction movement has a much lower amplitude compared to the flexion-extension ones.

Based on these exercises, the therapist looks for data related to grip and pinch strength, joint range of motion, and functional abilities (Dipietro L. et al., 2003). Their assessment provides key-information for diagnosis, rehabilitation program and treatment progress analysis.

The most common tactic to retrieve the required data is based on the measurement of the finger range of movements while the subject is grabbing different balls of different densities. For the range of movement is measured via a goniometer place on each finger joint which allied to the ball density enables the strength calculus. As one can imagine, such technique is

prone to errors, due to parallax effect, and inappropriate use of the equipment. Furthermore, such technique does not enable a simultaneous measurements of the entire had range of motion. As a result, the therapist takes a significant amount of time to perform all the required measurements that end up to have associated errors (Dipietro L. et al., 2003).

Independently of the performed exercises, the subjectivity associated to the patient's evaluation by the therapist leads to non-conclusive assessment of the patient's motor capacity and consequently misdiagnosis. Furthermore, the existing solutions are not suited to dynamic measurements. This scenario opens the opportunity for the development of a wearable device capable of performing an online monitoring of the hand kinematics in a more efficient manner.

3.2. State-of-the-art

In a generic scenario, a set of sensors applied to a glove are able to retrieve data related to the hand posture, from which directly or indirectly, depending on the sensor system architecture, other measurands can be also retrieved, e.g. pinch strength, motion range, among others (Dipietro L. et al., 2003).

It is already possible to find some wearable solutions capable of monitoring the hand posture and retrieving the required data, few based on electrically conductive elastomer (Lorussi F. et al., 2003; Lorussi F. et al., 2005; Scilingo E. P. et al., 2003; Tognetti A. et al., 2006), accelerometers (Perng J. K. et al., n.d.), induction coils, (Fahn C.-S. et al., 2005) and hetero-core fiber optic sensor (Nishiyama M. et al., 2009), but none on FBGs.

However, the available solutions are quite complex (Silva A. F. et al., 2011b), namely because of non-linear responses from the sensor, fragility issues or complex methods for signal processing. Still, from the existing technologies and solutions, the ones based on optical fiber sensors offer the biggest potential, when looking for performance and wearability (Lee B., 2003).

A solution based on FBG sensors can accomplish a simpler device compared to the existent ones by working on the sensor system design.

3.3. Monitoring approach

The finger movements on the joint site induce strain, namely tensile on the upper-side and compressive on the bottom-side, considering the open hand the steady-state. By applying a FBG on the joint site and use it as a strain gauge, one can related the measured strain to the angle between joints. The Bragg pitch deviates in accordance to the finger's flexion and extension movements.

A human hand has 14 joints to be monitor. Therefore, the same number of FBGs is required to be positioned at each joint. The FBGs' inherent multiplexing and self-referencing characteristics helps to reduce the system complexity as all the required sensors can be fitted in a single optical fiber (see the Figure 6).

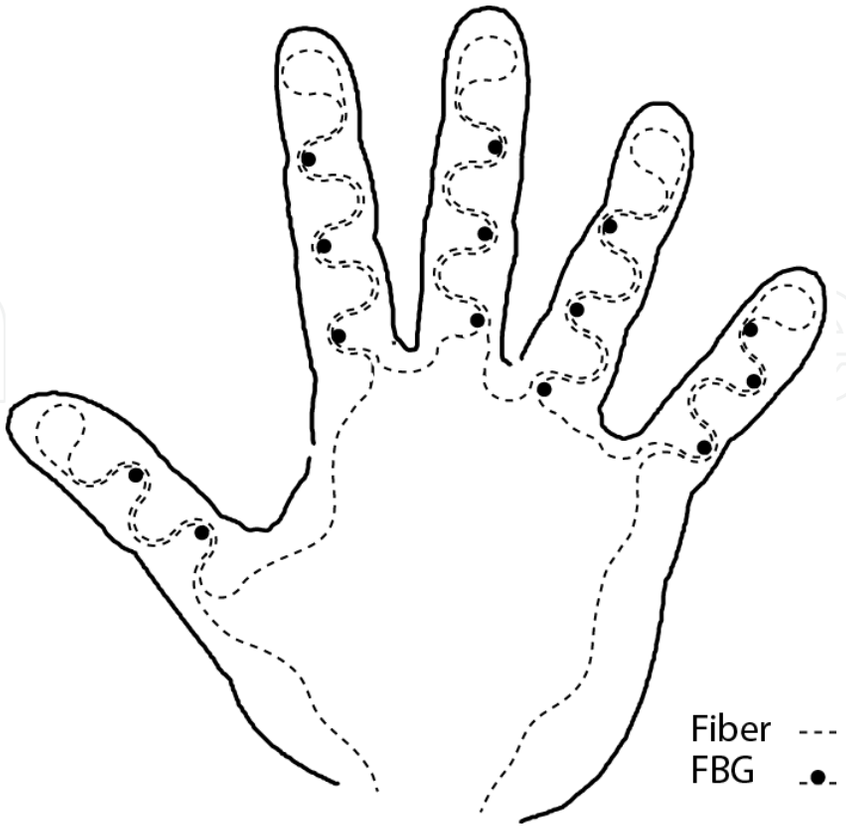

Figure 6. FBG sensor positioning proposal.

The nominal elongation of the finger joints, at the top or bottom face of the hand, is around 14 %, which is higher that the optical fiber's elongation range. Such limitation can be overcome in at least three methods by playing with the sensor positioning and/or optical fiber layout:

- The sensor may be placed on the side face of the joint. It is known that at a midline of a structure, the elongation while bending is null. A similar situation occurs on the finger joints, as one can see it as a bending load applied to the finger. Closer the FBG is positioned to the midline, lower is the strain that it will undergo. However, there is a trade-off associated to the movement sensitivity.
- The optical fiber can be coiled around the finger. This would create a spring effect on the optical fiber as the finger performs flexion and extension.
- Place the fiber in a curvilinear layout over the upper-face plane of the hand. This simulates the previous coil effects but on a two dimensional plane.

Based on the developed technique to integrate FBGs on flexible polymeric laminates, one could fabricate such laminate and use as a glove's upper face. On the upper face, the sensors are positively stretched, avoiding the wrinkles effect that occurs on the glove's lower face.

The laminate fabrication process ensures the correct positioning of the sensors and, at the same time, it provides protection to the optical fiber, enabling reliability and improving the wear out.

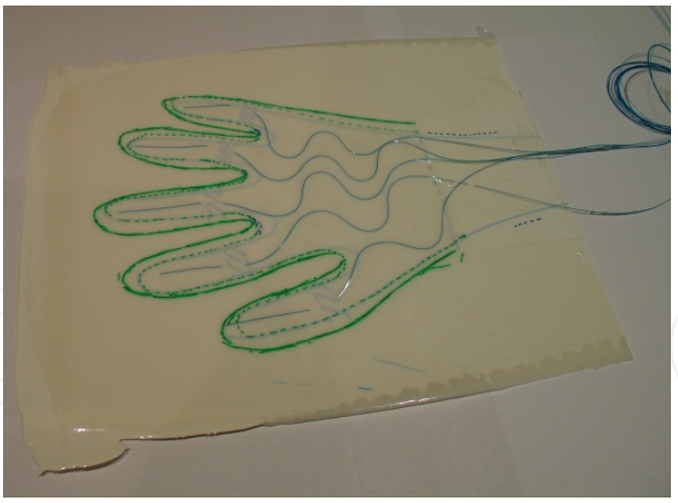

(a)

(b)

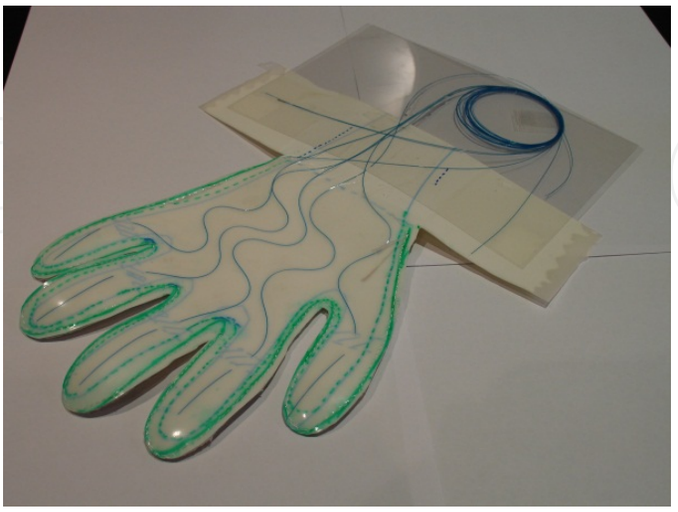

(c)

Figure 7. (a) Hand-shape polymeric foil with embedded FBGs; (b) Polymeric foil being sewed to a textile glove; (c) FBG-instrumented glove functional prototype.

3.4. Glove fabrication

Although the bare optical fiber commonly used for FBG only has an external diameter of 250 μm, which makes it perfect to be embedded in many structures, its fragility is still a major issue. The developed solution based on the integration of optical fiber and FBGs inside a thin and flexible polymeric substrate facilitates its use as a garment. It has been reported its flexibility, stretchability and capacity to keep the bond between the optical fiber and the substrate for signal transduction (Silva A. F. et al., 2009; Silva A. F. et al., 2010a). The degree of customization of the flexible substrate enables it to be manufactured with a hand shape. The approach was to replace the upper face of a glove by the polymeric substrate with the embedded FBGs in a single optical fiber (see the photographs in the Figure 7).

3.5. Performance assessment

The Figure 8 shows the raw signal obtained while the ring finger performs flexion and extension movements. The raw data shows the Bragg pitch deviation along the time the subject perform opening and closing hand movements. It is important to remark that the retrieved data is only related to the proximal interphalangeal crease of the ring finger. From the raw data, information can be processed namely, range of motion, strength and movement speed.

As the sensors are positioned on the glove's upper face, as the subject closes the hand, a positive strain occurs on the sensor site, resulting in a positive deviation of the Bragg pitch. As one opens the hand, the Bragg pitch decreases. For data processing, the null deviation occurs when the subject has his hand open, while the maximum deviation is set to the close hand state, driving the maximum strain.

Indirectly, the strength may be determined, since there is a correlation between the measured strain and the required load of 128 $pm.N^{-1}$ (Silva A. F. et al., 2010b).

An important characteristic in this type of systems is the accuracy. For this system, such parameter is evaluated comparing the value retrieved from the system with the valued measured by a goniometer. A FBG-based system is able to present an almost true linear response - see the Figure 8(b) - with a maximum error of 2º in a 90º range.

Although the system mainly monitors the flexion-extension movement, one could experience that the acquired data is not influenced by the abduction-adduction, as it is constrained by the glove's structure itself.

Another key factor while developing the sensing glove is related to the Bragg wavelength inscription for each one of the 14 FBGs sensors. The reflected spectral component of each FBG uses around 0.3 nm of the available spectrum and requires a dynamic range of 1 nm for the finger movement. By considering the C-band optical range (1530-1560 nm), each FBG should be inscribed in 1.84 nm steps in order to fit all sensors in a single fiber.

3.6. Virtual hand movement

The therapy session not only is tedious for the therapist as it also monotonous to the patient. In order to improve the motivation surrounding the therapeutic session, a virtual reality

environment may be set up based on the developed monitoring system. As the data that is retrieved from the sensors is made via personal computer, besides presenting the data exclusively for the therapist, the data can be used to create a tridimensional model of the hand that replicates what the patient is doing.

Furthermore, virtual interaction can be added, enabling game-like and personalized paced exercises to promote finger strength while keeping the subject motivated.

In the developed environment (see the Figure 9), it is possible to visualize the hand movement in real-time and provide at the same time information about the hand posture in terms of angles, strength and movement range.

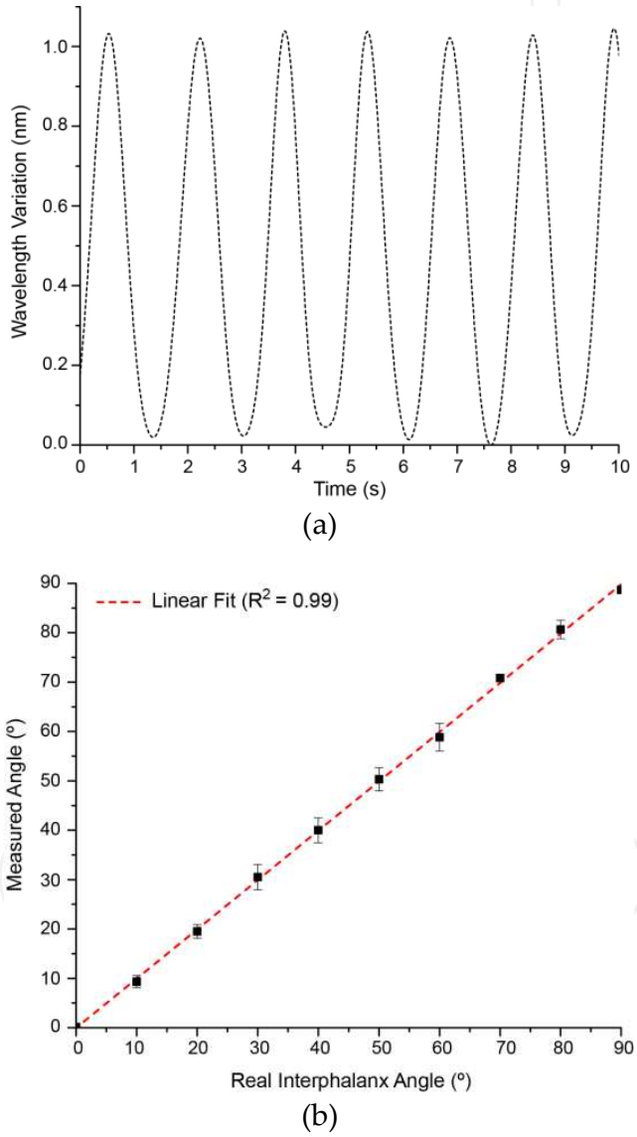

Figure 8. (a) Ring finger FBG sensor response for opening and closing hand movements; (b) System accuracy based on the comparison between real and measured angles.

A virtual monitoring system can be developed in LabView® environement with two purposes:

- Stimulate the patient to the therapy sessions by establishing game-like exercises. The hand movements are replicated in real time on the virtual environment that can be rotated and span.
- Provide information to the therapist regarding the angle at each joint, range of motion, movements speed and strength. It also provides a database of records that are helpful to evaluate the treatment evolution.

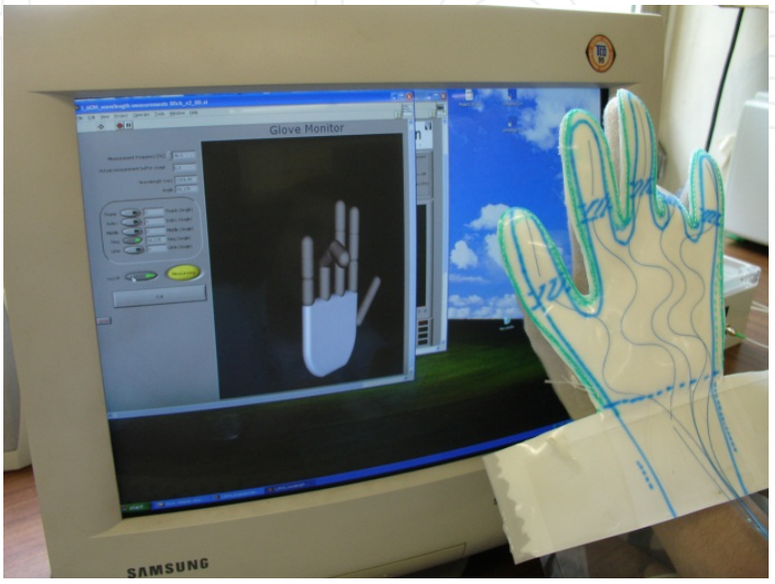

Figure 9. An example of the real-time monitor of the hand posture.

The monitoring hardware enables sampling frequencies from 32 Hz up to 2 kHz, ensuring a smooth visualization of the hand movement. The computational requirements are quite low (Intel Pentium IV processor with 512 MB of RAM), meaning that this systems does not require any special configuration, which is of great interest as it reduces the cost.

4. Cardio-respiratory frequency monitoring

The ability to monitor the vital signs of patients requiring medical assistance is a crucial issue (Fernandez R. et al., 2005), where the respiratory and the cardiac frequencies can be selected (among others) as presenting high interest (Evans D. et al., 2001). There are specific situations where the acquisition of these frequencies are important, e.g., with patients doing exams based on Magnetic Resonance Imaging (or MRI). However, this can be unsuitable, due to the potential occurrence of thermal or electrical burns associated with oximeter sensors and cables, temperature probes and MRI surface coils. These burns can be a result of inductions during MRI exams (Dempsey M. F. et al., 2001; Jones S. et al., 1996) or even during cardiothoracic surgeries (Wehrle G. et al., 2001). Therefore, the use of optical fibers can be an interesting solution for measuring the cardio-respiratory frequency. This statement is of particular importance because the optical fibers don't contain conductive parts therefore, this makes the optical fibers insensitive to external electromagnetic fields. In this section it will be proved the exequibility to deploy sensing/monitoring solutions for both the pulmonary and the cardiac frequency. Contrary to similar solutions found in the

literature (Augousti A. T. et al., 2005; Davis C. et al., 1999), this section shows how it is possible to use a single optical fiber sensor and at the same time keeping it compatible with the healthcare environments.

4.1. Approach

There are few requirements that must be addressed: providing a simple sensing solution capable of measuring the cardio-pulmonary components with a single sensor and at the same time ensures their compatibility with different people. As illustrated in the Figure 10, the most suitable approach for complying with these requirements is providing a small and flexible structure able to readily be attached/unattached to/from the chest's site. Such approach enables their use by any person. A fixation mechanism must also be provided in order to ensure that the sensing element is able to follow the elongation of the chest wall due to respiratory and cardiac components. This flexible structure is designated as carrier material and was used with the intention to increase the strain sensitivity of the FBG sensors, as well as, to improve the adhesion.

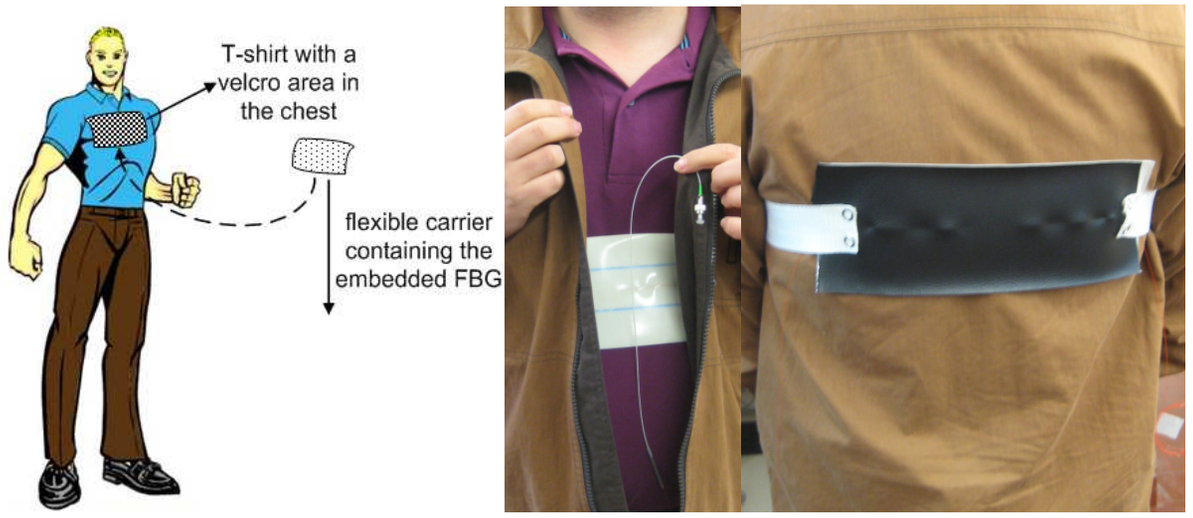

Figure 10. An illustration and two photographs with two views (the front and the backside views are respectively the left and right photographs) of the proposed approach showing the carriers containing the FBGs sensors.

4.2. Methodology

The Figure 11 shows a functional prototype that was tested on a group of few healthy subjects with ages between twenty and thirty years old. During the take of the measurements, the subjects were standing up and maintaining the full body to rest. It must be noted that the sensing foil was placed over the chest because this is the position of the human body where the effects of the heart beats are more significant.

The Figure 12 shows the block diagram of the complete FBG acquisition system. This filtering system was implemented for separating the respiratory and cardiac components from the acquired FBG signals. This system uses two band-pass filters, e.g., one is tuned in

the 0.1-0.4 Hz range for allowing the measurement of the respiratory frequency. The pass-band of the second filter rejects all spectral components, except those in the range 0.5-1.3 Hz for retrieving the cardiac frequency. This second band-pass filter allows the discrimination of frequency around 1 Hz. This set with the frequencies of interest are obtained by cutting the respiratory components below 0.5 Hz and the high frequencies (mainly composed by high frequency noise) above 1.3 Hz. A software application was used to implement both pass-band filters in the digital domain using the bilinear technique (Losada R. A. et al., 2005) with a sampling frequency of 36 Hz.

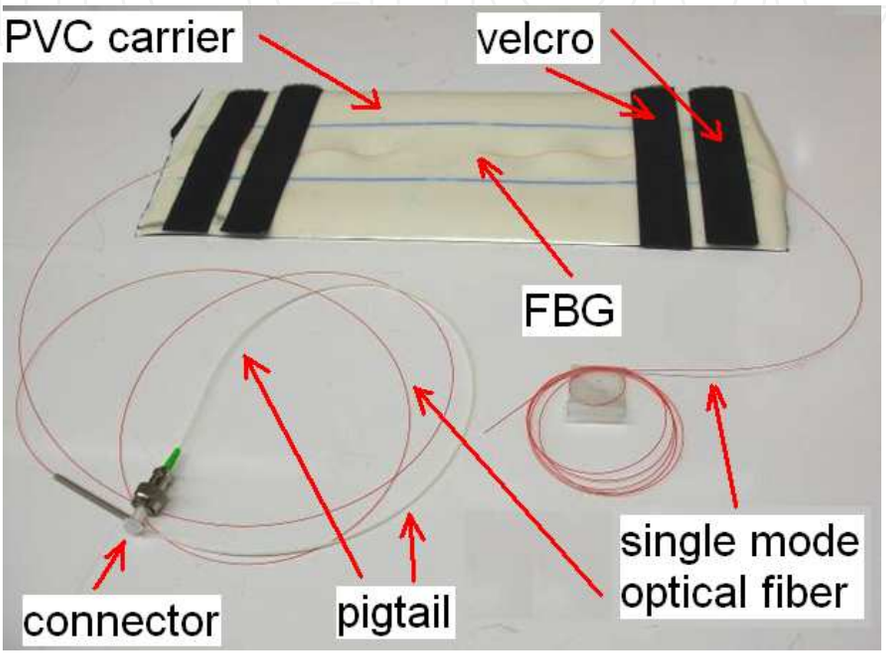

Figure 11. Photograph of a functional prototype (Silva A. F. et al., 2011a).

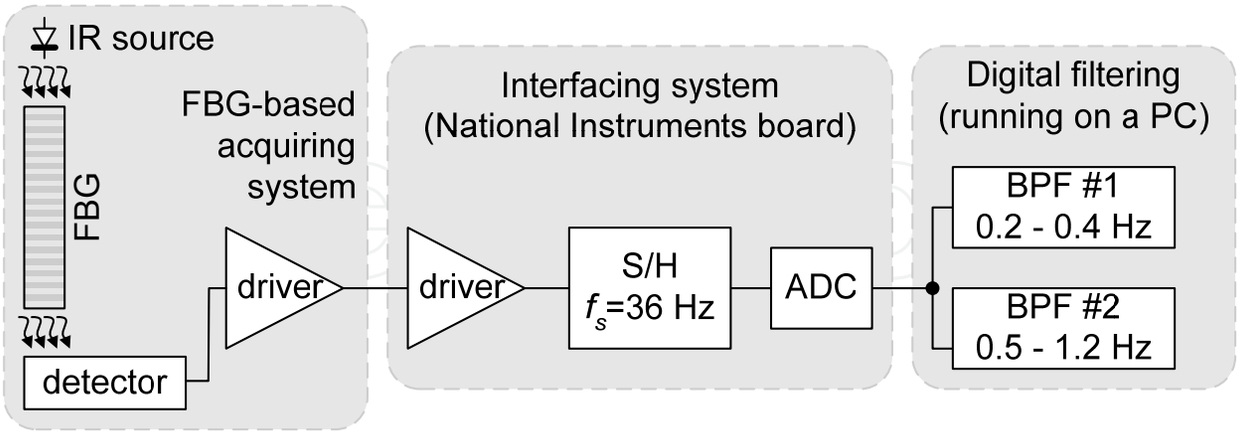

Figure 12. The block diagram of the FBG acquisition system (Silva A. F. et al., 2011a).

4.3. Experimental: Respiratory frequency

In the first trials, the subjects breathing naturally for evaluating the raw signal without any processing stage. As illustrated in the Figure 13, the external interferences do not appear to

degrade the quality of the acquired signals. The small perturbations that were observed are mainly due to the transition between the inhale and the exhale stages.

The ability to establish a relation between the wavelength deviation to other quantities (e.g., the displacement and force) is one advantage of these sensors and their linear response to strain. As the FBG spectral signature deviates 8 nm per 1% of elongation (Silva A. F. et al., 2010b), it is possible to retrieve how much did the chest stretched. Consequently, the air volume that is inhaled and exhaled can also be estimated as well as the force that is being applied to breath. As the chest elongation can be retrieved from the Bragg pitch deviation, the volume of air inhaled or exhaled can be determined, as the Bragg sensors responds linear to strain (Silva A. F. et al., 2011c). A similar approach can be used to obtain the applied load to inhale, since there is also a linear relationship between the elongation and the necessary load (Silva A. F. et al., 2010a). The Figure 14 shows the corresponding frequency spectrums, which confirms the existence of main frequency peak between 0.1 and 0.4 Hz. In this figure is also possible to observe the group of high-frequency components superimposed on the normal respiratory signal that may be originated from involuntary body movements.

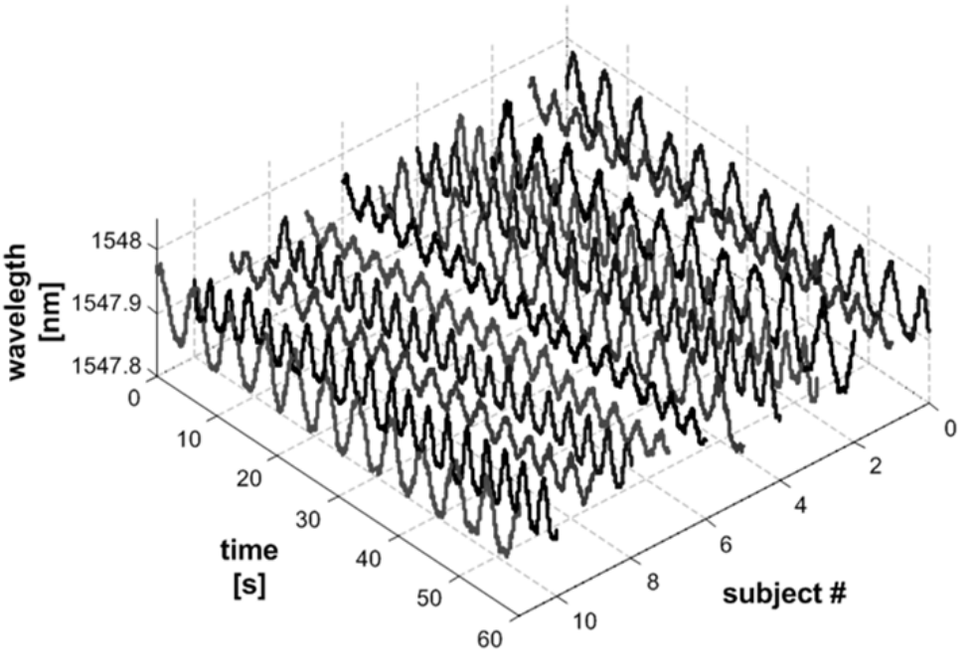

Figure 13. The sensor response to a normal breath (raw data) that was obtained for a group of twelve healthy subjects (#0 to #11).

These respiratory results were compared with reference signals acquired with the help of a commercial device (e.g., the Zephyr BioHarness) for validation purposes. The raw signals acquired from the FBGs were subjected to a band-pass filter in the 0.1-0.4 Hz range. The Figure 15 shows the signals of a single subject that have been acquired with the help of both the commercial device and the FBG sensor. It is possible to confirm quasi-identical behaviors along the time for the signals variations. However, a few differences may be due to the signal processing stage of the commercial device to which there was no access to.

Nevertheless, the same respiratory frequency (e.g., about 24 inhales per minute) was determined in both signals, and therefore, validating the measurements with FBGs.

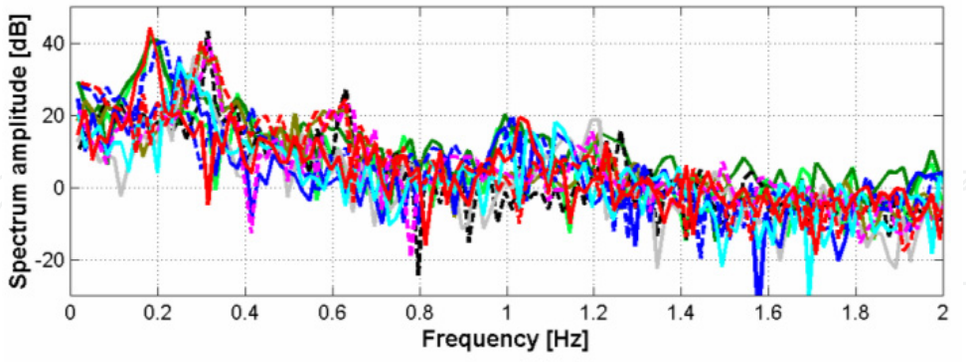

(a)

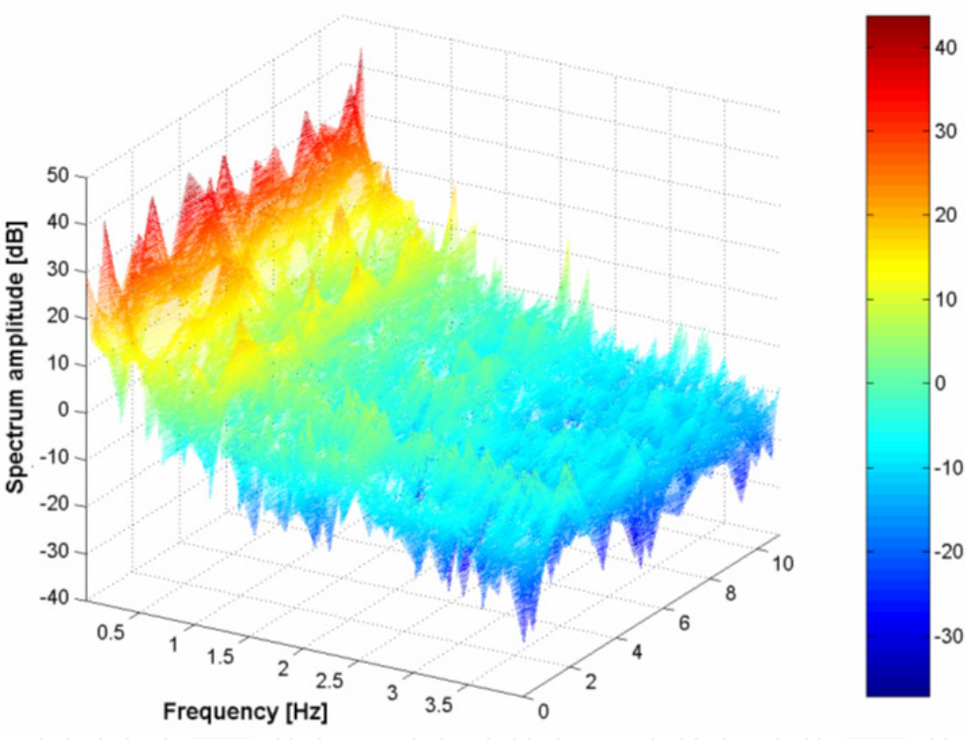

(b)

Figure 14. The frequency spectrum of normal breath also obtained for a group of twelve healthy subjects (#0 to #11). There top plot shows a superposition of all frequency spectrums for achieving a better visualization of the breading peaks. The bottom plot allows a better visualization of all frequency spectrums in the whole frequency range.

4.4. Experimental: Cardiac frequency

It exist a different test where the subjects are asked to do a deep inhale and a halt on its breath (once again, the Figure 16 shows an example for a single subject). At this point, a higher frequency response was obtained when compared with the respiratory frequency. The observation of these results led to the assumption that this behavior was related to the

heart beat frequency. The signals showed in the Figure 17 correspond to the cardiac part and were retrieved with the help of the signal processing stage illustrated in the Figure 12. The respective frequency spectrums are illustrated in the Figure 18, where it is a clear the existence of a region with the location of the cardiac frequency peaks in the range 0.5-1.3 Hz.

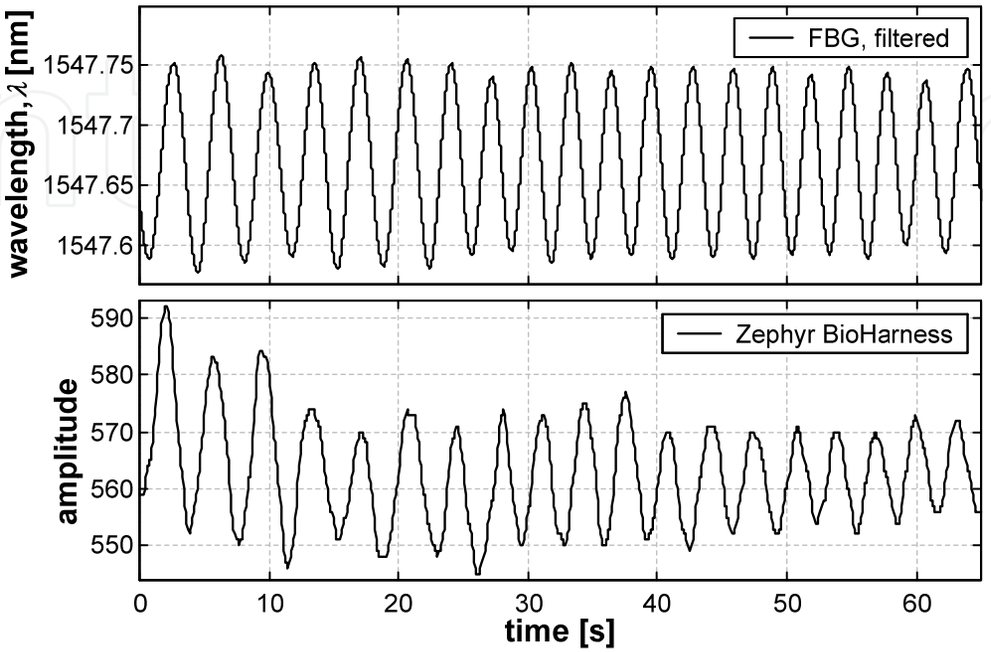

Figure 15. For the respiratory component: the FBG-based sensing structure response (plot on top) versus the Zephy BioHarness commercial response (plot on bottom).

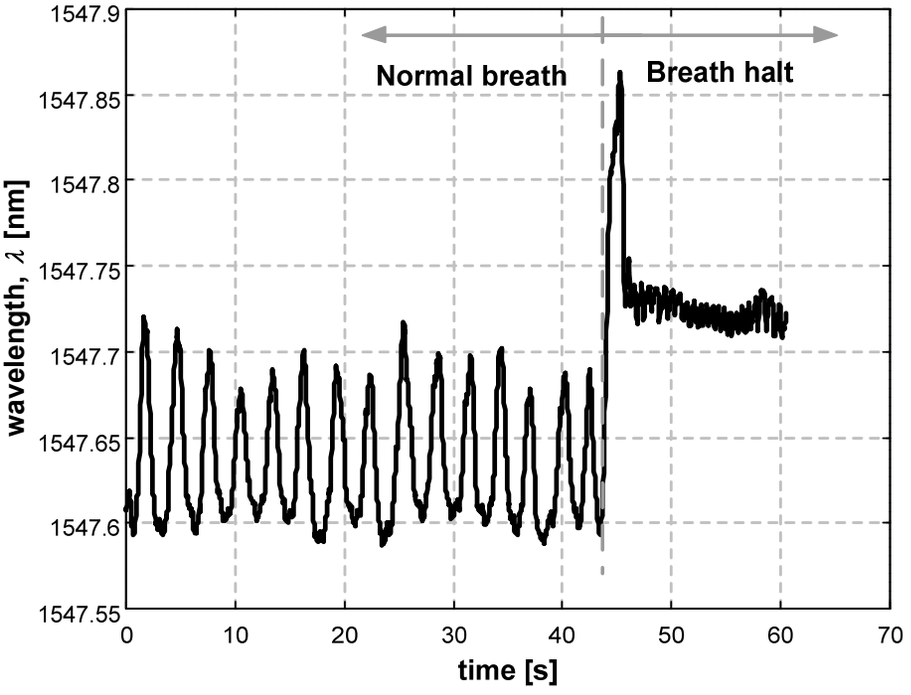

Figure 16. Sensor's response to a normal breath followed by a breath halt.

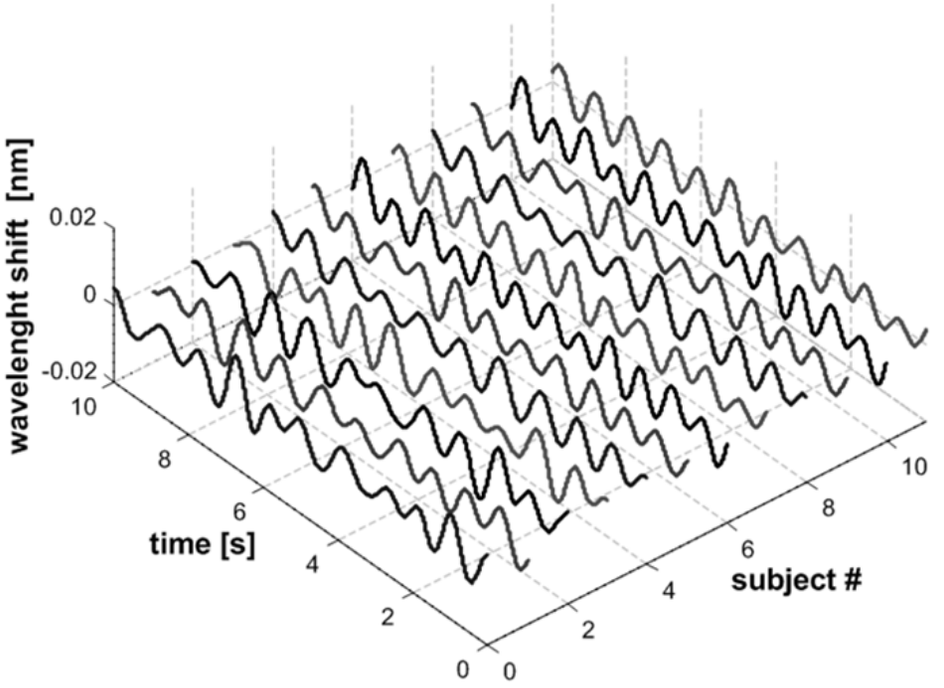

Figure 17. The cardiac frequency signals obtained by filtering the acquired raw data from the twelve healthy subjects (#0 to #11).

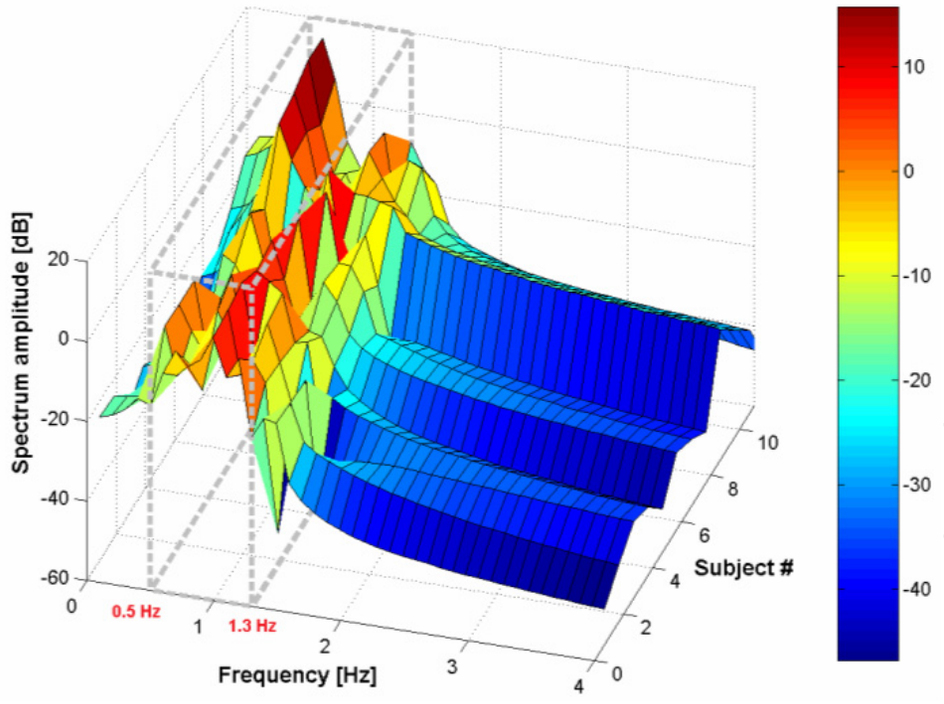

Figure 18. The frequency spectrum of the cardiac frequency for the twelve healthy subjects (#0 to #11).

The validation of the cardiac components was also done by comparing the obtained results with the commercial device previously used. The comparison between both systems is showed in the Figure 19. This test was also done for a single test subject because their cardiac frequency peaks are all located in the expected frequency range, e.g., between 0.5 Hz

and 1.3 Hz. The FBG sensor and the flexible carrier in PVC present a similar behavior in comparison with the commercial system, e.g., 66 heartbeats per minute on both. Therefore, this approach makes possible to retrieve the information about the cardiac frequency. It must be noted that some of the lag between the both signals is a result from external factors. Such factor includes involuntary movements and irregularities in the breath.

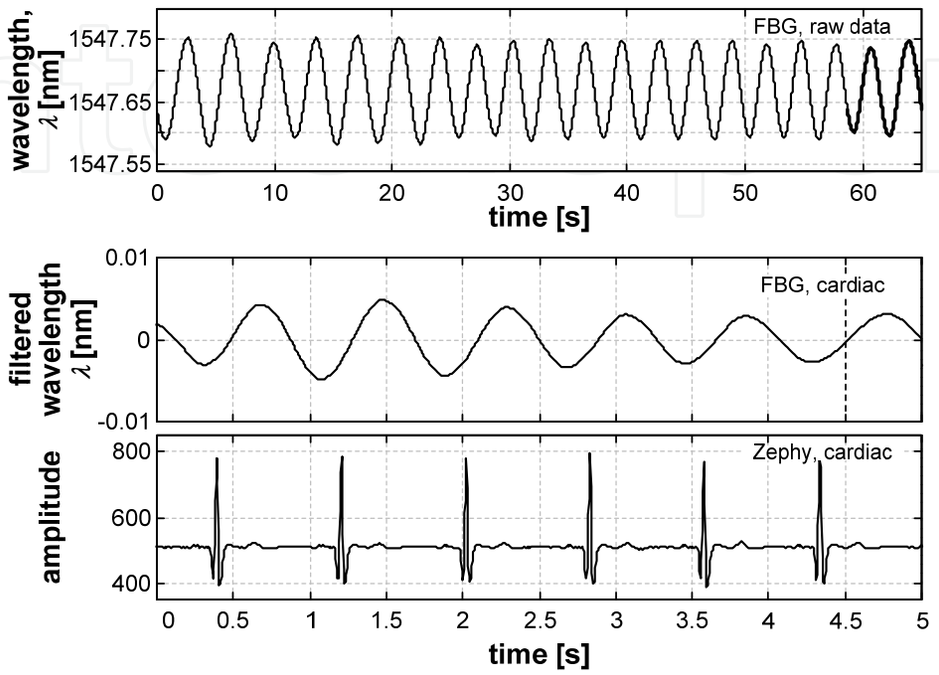

Figure 19. For the cardiac component retrieving: the FBG sensing structure raw data (top plot) and cardiac frequency (middle plot) and comparison with commercial system (bottom plot).

5. Epilogue

This chapter presented biomedical applications for acquisition systems based on FBGs. The absence of mechanical steps on sensor's fabrication results in the possibility to fabricate high sensitivity sensors with high reproducibility of their characteristics (Hill K. O. *et al*., 1997). However, the most important features that made FBG-based systems a wide established technology were their electrically passive operation, electromagnetic interference immunity, compact size, self referencing capability, and more important, inherent multiplexing-ability, which enable a wide number of sensors in a single fiber as well as Bragg a single interrogation system (Wang Q. *et al*., 2007). In conclusion, the FBGs are not restricted for the applications presented in this chapter.

Author details

Alexandre Ferreira da Silva
MIT Portugal Program, School of Engineering, University of Minho, Guimarães, Portugal

Rui Pedro Rocha, João Paulo Carmo and José Higino Correia
Department of Industrial Electronics, University of Minho, Guimarães, Portugal

Acknowledgement

This work was fully supported by the Algoritmi's Strategic Project UI 319-2011-2012, under the Portuguese Foundation for Science and Technology grant Pest C/EEI/UI0319/2011. Furthermore, the PhD student Rui Pedro Rocha was fully supported by the PhD scholarship with the reference SFRH/BD/33733/2009.

6. References

Afonso, J. A., Macedo, P., Silva, H. D., Correia, J. H., Rocha, L. A. (2010). "Design and Implementation of Multi-User Wireless Body Sensor Networks", *Journal on Advances in Networks and Services, IARIA Publisher,* 3(*1&2*): 62-74.

Alton, F., Baldey, L., Caplan, S., Morrissey, M.C. (1998). "A kinematic comparison of overground and treadmill walking", *Clinical Biomechanics,* 13(*6*): 434-440.

Anderson, D., Sidaway, B. (1994). "Coordination changes associated with practice of a soccer kick", *Research Quarterly Exercise and Sport,* 65(*2*): 93-99.

Antunes, P., Varum, H., and André, P. (2011). Uniaxial fiber Bragg grating accelerometer system with temperature and cross axis insensitivity", *Measurement*, 44(*1*): 1-5.

Arregui, F. J., Matias, I. R., Cooper, K. L., and Claus, R. O. (2002). Simultaneous measurement of humidity and temperature by combining a reflective intensity-based optical fiber sensor and a fiber bragg grating, *IEEE Sensors Journal*, 2(*5*): 482-487.

Augousti, A. T., Maletras, F. X., and Mason, J. (2005). Improved fibre optic respiratory monitoring using a figure-of-eight coil, *Physiological Measurement*, 26(*5*): 585-590.

Bao, H., Dong, X., Zhao, C., Shao, L. Y., Chan, C. C., and Shum, P. (2010). Temperature insensitive FBG tilt sensor with a large measurement range, *Optics Communications*, 283(*6*): 968-970.

Beard, P. C., Mills, T. N. (1996). "Extrinsic optical-fiber ultrasound sensor using a thin polymer film as a low-finesse Fabry-Perot interferometer", *Applied Optics,* 35(*4*): 663-675.

Bilro, L., Oliveira, J. G., Pinto, J. L., Nogueira, R. N. (2011). "A reliable low-cost wireless and wearable gait monitoring system based on a plastic optical fibre sensor", *Measurement Science and Technology,* 22(*4*): 1-7. Institute of Physics Paper 045801.

Boerkamp, M., Lamb, D. W., Lye, P. G. (2007, July). "Using an intrinsic, exposed core, optical fibre sensor to quantify chemical scale formation", *Journal of Physics: Conference Series,* 76(*1*): 1-7. Institute of Physics Paper 012016.

Carmo, J. P., Silva, A. F., Rocha, R. P., and Correia, J. H. (2012). Application of fiber Bragg gratings to wearable garments, *IEEE Sensors Journal*, 12(*1*): 261-266.

Cup, E. H., Pieterse, A. J., ten Broek-Pastoor, J. M., Munneke, M., van Engelen, B. G., Hendricks, H. T., van der Wilt, G. J., Oostendorp, R. A. (2007). "Exercise therapy and other types of physical therapy for patients with neuromuscular diseases: A systematic review", *Archives of Physical Medicine and Rehabilitation,* 88(*11*): 1452-1464.

Davis, C., Mazzolini, A., Mills, J., and Dargaville, P. (1999). A new sensor for monitoring chest wall motion during high-frequency oscillatory ventilation, *Medical Engineering & Physics*, 21(*9*): 619-623.

Dempsey, M. F., and Condon, B. (2001). Thermal injuries associated with MRI, *Clinical Radiology*, 56(*6*): 457-465.

Denselight Semiconductors. (2012). [on-line, 25th June 2012]: http://www.denselight.com/.

Dipietro, L., Sabatini, A. M., and Dario, P. (2003). "Evaluation of an instrumented glove for hand-movement acquisition", *Journal of rehabilitation research and development*, 40(*2*): 179-189.

Evans, D., Hodgkinson, B., and Berry, J. (2001). Vital signs in hospital patients: a systematic review, *International Journal of Nursing studies*, 38(*6*): 643-650.

Fahn, C.-S., and Sun, H. (2005). "Development of a data glove with reducing sensors based on magnetic induction", *IEEE Transactions on Industrial Electronics*, 52(*2*): 585-594.

Fender, A., MacPherson, W. N., Maier, R., Barton, J. S., George, D. S., Howden, R. I., Smith, G. W., Jones, B. McCulloch, S., Chen, X., Suo, R., Zhang, L., and Bennion, I. (2008). Two-axis temperature-insensitive accelerometer based on multicore fiber bragg gratings, *IEEE Sensors Journal*, 8(*7*): 1292-1298.

Fernandez, R., and Griffiths, R. (2005). A comparison of an evidence based regime with the standard protocol for monitoring postoperative observation: a randomised controlled trial, *The Australian journal of advanced nursing: a quarterly publication of the Royal Australian Nursing Federation*, 23(*1*): 15-21.

FiberSensing Sistemas Avançados de Monitorização, S. A. (2012). [on-line, 25th June 2012]: http://www.fibersensing.com/.

Godfrey, A., Conway, R., Meagher, D., and ÓLaighin, G. (2008). "Direct measurement of human movement by accelerometry", *Medical Engineering & Physics*, 30(*10*): 1364-1386.

Grattan, S. K. T., Taylor, S. E., Sun, T., Basheer, P. A. M., and Grattan, K. T. V. (2009). "In-situ cross-calibration of in-fiber bragg grating and electrical resistance strain gauges for structural monitoring using an extensometer", *IEEE Sensors Journal, 9*(*11*): 1355-1360.

Grillet, A., Kinet, D., Witt, J., Schukar, M., Krebber, K., Pirotte, F., and Depré, A. (2008). "Optical fiber sensors embedded into medical textiles for healthcare monitoring", *IEEE Sensors Journal*, 8(*7*): 1215-1222.

Gu, X., Guan, L., He, Y., Zhang, H. B., and Herman, P. R. (2006). High-strength fiber bragg gratings for a temperature-sensing array, *IEEE Sensors Journal*, 6(*3*): 668-671.

Hill, K. O., and Meltz, G. (1997). Fiber Bragg grating technology fundamentals and overview, *IEEE Journal of Lightwave Technology*, 15(*8*): 1263-1276.

Ibsen Photonics. (2012). [on-line, 25th June 2012]: http://www.ibsen.dk/.

Jones, S., Jaffe, W., and Alvi, R. (1996). Burns associated with electrocardiographic monitoring during magnetic resonance imaging. Jo*urnal of the International Society for Burn Injuries*, 22(*5*): 420-421.

Kang, H. G., and Dingwell, J. B. (2008). "Separating the effects of age and walking speed on gait variability", *Gait & Posture*, 27(*4*): 572-577.

Kun, L., Inoue, Y., Shibata, K., and Enguo, C. (2011). "Ambulatory estimation of knee-joint kinematics in anatomical coordinate system using accelerometers and magnetometers", *IEEE Transactions on Biomedical Engineering*, 58(*4*): 435-442.

Lee, B. (2003). "Review of the present status of optical fiber sensors", *Optical Fiber Technology*, 9(*2*): 57-79.

Ling, H. Y., Lau, K. T., Cheng, L., and Jin, W. (2006). Viability of using an embedded FBG sensor in a composite structure for dynamic strain, *Measurement*, 39(*4*):328-334.

Lloyd-Jones, D., Adams, R. J., Brown, T. M., Carnethon, M., Dai, S., De Simone, G., Ferguson, T. B., et al. (2010). "Heart Disease and Stroke Statistics 2010 Update: a Report from the American Heart Association", *Circulation*, 121: 173.

Lorussi, F., Scilingo, E. P., Tesconi, A., Tognetti, A., and De Rossi, D. (n.d.). Wearable sensing garment for posture detection, rehabilitation and tele-medicine, Proceedings of the 4th International IEEE EMBS Special Topic Conference on Information Technology Applications in Biomedicine, 287-290.

Lorussi, F., Scilingo, E. P., Tesconi, M., Tognetti, A., and De Rossi, D. (2005). "Strain sensing fabric for hand posture and gesture monitoring", *IEEE transactions on information technology in biomedicine*, 9(*3*): 372-381.

Losada, R. A., and Pellisier, V. (2005). Designing IIR filters with a given 3-dB point, *IEEE Signal Processing Magazine*, 22(*4*):95-98

Mavrogiorgoua, P., Mergla, R., Tiggesa, P., Husseinia, J., Schrötera, A., Juckela, G., Zaudigb, M., and Hegerla, U. (2001). "Kinematic analysis of handwriting movements in patients with obsessive-compulsive disorder", *Journal of Neurology, Neurosurgery & Psychiatry*, 70(*5*): 605-612.

Moustakidis, S. P., Theocharis, J. B., and Giakas, G. (2010). "A fuzzy decision tree-based SVM classifier for assessing osteoarthritis severity using ground reaction force measurements", *Medical Engineering & Physics*, 32(*10*): 1145-1160.

Nishiyama, M., and Watanabe, K. (2009). "Wearable sensing glove with embedded hetero-core fiber-optic nerves for unconstrained hand motion capture", *IEEE Transactions on Instrumentation and Measurement*, 58(*12*): 3995-4000.

Oplink Communications Inc. (2012). [on-line, 25th June 2012]: http://www.oplink.com/.

Orr, P., and Niewczas, P. (2010). An optical fiber system design enabling simultaneous point measurement of magnetic field strength and temperature using low-birefringence FBGs, *Sensors and Actuators A*: *Physical Sensors*, 163(*1*): 68-74.

Parker, T. M., Osternig, L. R., van Donkelaar, P., and Chou, L.-S. (2008). "Balance control during gait in athletes and non-athletes following concussion", *Medical Engineering & Physics*, 30(*8*): 959-967.

Patterson, K. K., Nadkarni, N. K., Black, S. E., and McIlroy, W. E. (2012). "Gait symmetry and velocity differ in their relationship to age", *Gait & Posture*, 35(*4*): 590-594.

Peng, B. J., Zhao, Y., Yang, J., and Zhao, M. (2005). Pressure sensor based on a free elastic cylinder and birefringence effect on an FBG with temperature-compensation, *Measurement*, 38(*2*): 176-180.

Peng, B.-J., Zhao, Y., Zhao, Y., and Yang, Y. (2006). Tilt sensor with FBG technology and matched FBG demodulating method, *IEEE Sensors Journal*, 6(*1*): 63-66.

Perng, J. K., Fisher, B., Hollar, S., and Pister, K. S. J. (n.d.). Acceleration sensing glove (ASG), Proceedings of the 3rd International Symposium on Wearable Computers.

Rajan, G., Callaghan, D., Semenova, Y., McGrath, M., Coyle, E., and Farell, G. (2010). A fiber bragg grating-based all-fiber sensing system for telerobotic cutting applications, *IEEE Sensors Journal*, 10(*12*): 1913-1919.

Ren, L., Jones, R. K., and Howard, D. (2008). "Whole body inverse dynamics over a complete gait cycle based only on measured kinematics", *Journal of Biomechanics,* 41(*12*): 2750-2759.

Riley, P. O., Paolini, G., Croce, U., Paylo, K. W., and Kerrigan, D. C. (2007). "A kinematic and kinetic comparison of overground and treadmill walking in healthy subjects", *Gait & Posture,* 26(*1*): 17-24.

Rocha, R. P., Silva, A. F., Carmo, J. P., and Correia, J. H. (2011). FBG Sensor for measuring and recording the knee joint movement during gait, Proceedings of the 33rd Annual International Conference of the IEEE Engineering in Medicine and Biology Society (EMBC '11), Boston, Massachusetts, USA.

Scilingo, E. P., Lorussi, F., Mazzoldi, a., and De Rossi, D. (2003). "Strain-sensing fabrics for wearable kinaesthetic-like systems", *IEEE Sensors Journal*, 3(*4*): 460-467.

Silva, A F, Goncalves, F., Ferreira, L. A., Araújo, F. M., Dias, N. S., Carmo, J. P., Mendes, P. M., and Correia, J. H. (2009). Manufacturing technology for flexible optical sensing foils, Proceedings of the 35th Annual Conference of IEEE Industrial Electronics (IECON 2009), Oporto, Portugal.

Silva, A. F., Gonçalves, F., Ferreira, L. A., Araújo, F. M., Mendes, P. M., and Correia, J. H. (2010a). "Fiber Bragg grating sensors integrated in polymeric foils", *Materials Science Forum*, 636-637: 1548-1554.

Silva, A. F., Goncalves, A. F., Ferreira, L. A., Araujo, F. M., Mendes, P. M., and Correia, J. H. (2010b). PVC smart sensing foil for advanced strain measurements, *IEEE Sensors Journal*, 10(*6*): 1149-1155.

Silva, A. F., Carmo, J. P., Mendes, P. M., and Correia, J. H. (2011a). Simultaneous cardiac and respiratory frequency measurement based on a single fiber Bragg grating sensor, *Measurement Science and Technology*, 22(*7*): 1-5. Institute of Physics Paper 075801.

Silva, A. F., Goncalves, A. F., Mendes, P. M., and Correia, J. H. (2011b), FBG sensing glove for monitoring hand posture, *IEEE Sensors Journal*, 11(*10*): 2442-2448.

Silva, A. F., Goncalves, A. F., Ferreira, L. A., Araujo, F. M., Mendes, P. M., and Correia, J. H. (2011c). A Smart skin PVC foil based on FBG sensors for monitoring strain and temperature, *IEEE Transactions on Industrial Electronics*, 58(*7*): 2728-2735.

Silva, A. F., Gonçalves, A. F., Mendes, P. M., and Correia, J. H. (2012). PVC formulation study for the manufacturing of a skin smart structure based in optical fiber elements, *Journal Polymers for Advanced Technologies*, *Wiley Publisher*, 23(*2*), 220-227.

Thorlabs GmbH. (2012). [on-line, 25th June 2012]: http://www.thorlabs.de/.

Tognetti, A., Carbonaro, N., Zupone, G., and De Rossi, D. (2006). Characterization of a novel data glove based on textile integrated sensors, Proceedings of the Annual International Conference of the IEEE Engineering in Medicine and Biology Society.

Trew, M., and Everett, T. (2005). Human movement: an introductory text, 5th edition. Elsevier Limited.

Turcot, K., Aissaoui, R., Boivin, K., Pelletier, M., Hagemeister, N., and Guise, D. (2008). "New accelerometric method to discriminate between asymptomatic subjects and patients with medial knee osteoarthritis during 3-D gait", *IEEE Transactions on Biomedical Engineering*, 55(*4*): 1415-1422.

Vancampfort, D., M. Probst, Skjaerven, L. H., Catalán-Matamoros, D., Lundvik-Gyllensten, A., Gómez-Conesa, A., Ijntema, R., and De Hert, M. (2012). "Systematic review of the benefits of physical therapy within a multidisciplinary care approach for people with schizophrenia", *Journal of the American Physical Therapy Association*.

von Porat, A., Henriksson, M., Holmström, E., and Roos, E. M. (2007). "Knee kinematics and kinetics in former soccer players with a 16-year-old ACL injury - the effects of twelve weeks of knee-specific training", *BMC Musculoskeletal Disorders,* 8(*35*).

Wang, Q., Rajan, G., Wang, P., and Farrell, G. (2007). Macrobending fiber loss filter, ratiometricwavelength measurement and application, *Measurement Science Technology*, 18(*10*): 3082-3088.

Wehrle, G., Nohama, P., Kalinowski, H. J., Torres, P. I., and Valente, L. C. G. (2001). A fibre optic Bragg grating strain sensor for monitoring ventilatory movements, *Measurement Science and Technology*, 12(*7*): 805-809.

Wei, C.-L., Lai, C.-C., Liu, S.-Y., Chung, W., Ho, T., Ho, S., McCusker, A., Kam, J., and Lee, K. (2010). "A fiber bragg grating sensor system for train axle counting". *IEEE Sensors Journal,* 10(*12*): 1905-1912.

Wu, Y., and Shi, L. (2011). "Analysis of altered gait cycle duration in amyotrophic lateral sclerosis based on nonparametric probability density function estimation", *Medical Engineering & Physics,* 33(*3*): 347-355.

Xie, F., Chen, Z., and Ren, J. (2009). Stabilisation of an optical fiber Michelson interferometer measurement system using a simple feedback circuit, *Measurement*, 42(*9*): 1335-1340.

Yamamoto, Y. (2004). "An alternative approach to the acquisition of a complex motor skill: Multiple movement training on tennis strokes", *International Journal of Sport and Health Science,* 2: 169-179.

Yang, X. J., Hill, K., Moore, K., Williams, S., Dowson, L., Borschmann, K., Simpson, J. A., and Dharmage, S. C. (2012). "Effectiveness of a targeted exercise intervention in reversing older people's mild balance dysfunction: a randomized controlled trial", *Journal of the American Physical Therapy Association*.

Yao, S.-K., and Asawa, C. (2003). "Fiber Optical Intensity Sensors", *IEEE Journal on Selected Areas in Communications,* 1(*3*): 562-575.

Yavuzer, G., Öken, Ö., Elhan, A., and Stam, H. J. (2008). "Repeatability of lower limb three-dimensional kinematics in patients with stroke", *Gait & Posture,* 27(*1*): 31-35.

Yeo, T. L., Sun, T., Grattan, T. K. V., Parry, D., Lade, R., and Powell, B. D. (2005). Polymer-coated fiber Bragg grating for relative humidity sensing, *IEEE Sensors Journal*, 5(*5*): 1082-1089.

Zhang, W., Li, F., and Liu, Y. (2009). FBG pressure sensor based on the double shell cylinder with temperature compensation, *Measurement*, 42(*3*): 408-411.

Zhao, Y., Zhao, Y., and Zhao, M. (2005). Novel force sensor based on a couple of fiber Bragg gratings, *Measurement*, 38(*1*): 30-33.